# Embedded Inertial Measurement Unit for Real-Time Sensor Integration and Data Processing

Andreas Fink, Christian Schröder, Andy Schellin, Helmut Beikirch
Department of Computer Science and Electrical Engineering
Rostock University
A.-Einstein-Str.2, 18059 Rostock, Germany
Email: {andreas.fink | christian.schroeder | andy.schellin | helmut.beikirch}@uni-rostock.de

***Abstract*—The latest advances in micro-electro-mechanical (MEMS) acceleration and gyroscopic sensors support the design of a low-cost and miniaturized inertial measurement unit (IMU). A custom MEMS-based IMU using a three-axis accelerometer, a three-axis gyroscope and a fluxgate magnetometer is proposed. Beside the noise characteristics of the IMU sensors, the sensor integration and data processing in real-time are the main issues to enable low INS position drifts. The digital processing unit (DPU) is based on the MSP430 architecture, offering a low-power controller core for real-time data processing (e.g. for Kalman filter, attitude and heading calculation, coordinate transformation, sensor fusion). A step detection framework for hip-mounted sensors is proposed and evaluated by experimental results of a tracking measurement in an office building.**

***Index Terms*—Inertial Measurement Unit, Inertial Navigation, MEMS, Pedestrian Navigation.**

## I. Introduction

For a reliable and precise positioning of people and materials in indoor multipath environments, it is a common technique to combine the position estimations of an RF-based localization system with an inertial navigation system (INS) [1]. Typical evaluation criteria for a taxonomy of an indoor local positioning system (ILPS) are given in [2] together with the general characterization of an ILPS.

Due to multipath fading, RF-based systems have a limited short-term accuracy in obstructed indoor environments. The main drawback of MEMS-based INS systems is the limited long-term stability due to error propagation of the direction and distance measurements. With a sensor fusion using e.g. a Kalman filter, the hybrid system offers both, a good short-term accuracy and a good long-term stability.

In section II, related MEMS-based position estimation techniques are discussed. The proposed IMU architecture is presented in section III. In section IV, the calibration of the MEMS acceleration and angular rate sensors is given. In section V, we validate the system's performance by experimental results of a step detection measurement inside our institute building. In the last section VI, the results are discussed and investigated in terms of an outlook for further system developments.

## II. Related Work

There are a lot of scientific papers dealing with the topic of pedestrian dead reckoning (PDR). MEMS-based acceleration sensors are usually used for acceleration measurements that enable a step detection [3],[4],[5]. Other systems use some additional classes of inertial sensors like gyroscopes [6]. A combination of three classes of IMU sensors in one strapdown system with 9 degrees of measurement (DOM) using a three-axis accelerometer, a three-axis gyroscope and a three-axis magentometer is described in [7]. An overview and a performance comparison of typical MEMS-based IMUs is given in [8]. Because of the large amount of scientific papers about this topic, it can be referred to some representative publications at this point.

In the following, a brief summary of the two major inertial localization techniques is given. The easiest way to calculate a covered distance, is to double integrate a measured acceleration as shown in (1).

$$x(t_0, t_1) = \int_{t_0}^{t_1} \left( \int_{t_0}^{t_1} a(t)dt \right) dt \tag{1}$$

The major disadvantage of this method is that offset or scaling errors as well as temperature dependencies and sensor noise have a large influence on the calculation results. Due to the double integral, a single error in the acceleration measurement will become a quadratic factor, so that even small errors have a great impact with error propagation over time.

Another approach to calculate a covered distance is offered by the step detection that is also known as pedometry. With a known step length $l$ and the number of steps $n$ it is possible to calculate the covered distance $d$ using (2).

$$s = n \cdot l \tag{2}$$

## III. IMU Architecture

The prototype of the embedded hardware platform for the localization system with the inertial measurement unit (IMU) using sensors from STMicroelectronics is shown in Fig. 1.

### A. Motion Sensors

In the middle of the PCB, the L3G4200D is placed, which is a low-power 3D angular rate sensor with various digital communication interfaces like SPI and I2C. The 3D acceleration sensor LIS3DH is placed below the angular rate sensor on top of the PCB. Details of the sensor's characteristics can be found in [9] and [10].

978-1-4673-1954-6/12/$31.00 

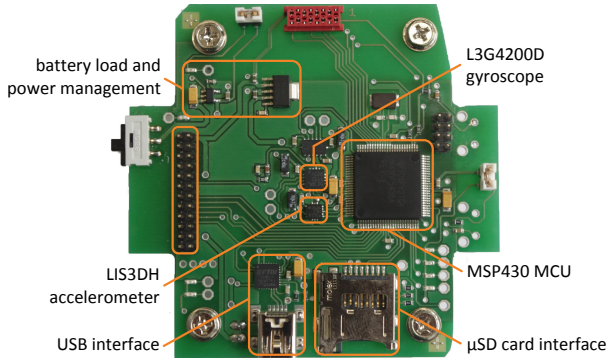


Fig. 1. Printed circuit board and IMU architecture containing motion sensors, microcontroller unit and communication interfaces.

### B. Microcontroller Unit (MCU)

The mircocontroller unit (MCU) is based on a Texas Instruments MSP430F5438A which has the best performance within the MSP430-family. The maximum frequency of the controller is $25\,MHz$ and it has $256\,KB$ flash and $16\,KB$ SRAM that can be used. Four universal serial communication interfaces (USCI) can be configured as SPI-, I2C- or UART-interfaces. They provide eight different digital interfaces.

### C. Additional Hardware

A $\mu$SD-card has been integrated in order to store the measurement data locally on the prototype. The controller is able to write the measurement data FAT compatible to the SD-card using an integrated FAT-library. Thus the data can be easily analyzed with a PC. This mode is a great advantage especially during the calibration stage. However, in normal operation the data will be transmitted to a data concentrator via radio frequency (RF) interface. For this purpose the prototype has a stack-based design. There is another PCB with a similar stack size and design available that includes an additional MSP430F5438A MCU and four proprietary RF modules (868 MHz / 2.4 GHz) [11].

The two MCUs communicate via SPI with each other so that the IMU-Data can be sent via RF frontend to the data concentrator PC. To guaranty an independent energy supply, the embedded system is powered through a lithium-polymer-battery with a nominal energy of about $5.18\,Wh$. A low dropout regulator (LDO) reduces the battery voltage to the desired operating voltage of $3.3\,V$. To recharge the battery, when the system is connected to an external power supply, a recharging circuit was integrated. Thanks to an USB-Port it is possible to recharge the system while being connected to the data concentrator PC.

## IV. Sensor Calibration

Although the inertial sensors are delivered as pre-calibrated by the manufacturer, a new calibration is required after the assembling because it is possible that the PCB is tilted or the sensors are not straight soldered.

A well known error compensation method for sensors is the two-point-calibration [12]. It allows to calculate the offset and scale factor by determining sensor data of known measure points and insert them into the general two-point-equation from (3). This implies that the process between the two points is linear.

$$y - y_1 = \frac{y_2 - y_1}{x_2 - x_1}(x - x_1) \tag{3}$$

In (3), $y$ stands for the sensor output, $y_1$ is the output at measure point $x_1$, $y_2$ is the output at measure point $x_2$ and $x$ is the value to be measured. The offset can then be determined with (4) if $x$ in (3) is set to zero.

$$offset = \frac{y_2 - y_1}{x_2 - x_1}(-x_1) + y_1 \tag{4}$$

The scaling factor $k$ can be calculated with (5).

$$k = \frac{x_2}{y_2 - T_{Offset}} \tag{5}$$

The compensation using (6) must be applied to correct the sensor values.

$$T_k = (T_m - T_{Offset}) \cdot k \tag{6}$$

### A. Calibration of the acceleration sensor

To calibrate the acceleration sensor the well known six-position-static-test [8] was applied. For this purpose, each side of the device is placed with the surface downward on a solid table. By this procedure, every sensitive axis of the accelerometer is exposed to the positive and negative acceleration of gravity. This procedure delivers reproducible results since the measuring range is clearly defined by $\pm 1\,g$.

The LIS3DH is set to $\pm 2\,g$ measuring range at a resolution of $12\,bit$. Ideally, this should lead to a digital value of $\pm 1024\,LSB$ at an acceleration of $\pm 1\,g$. Every position is at least kept for $20\,s$. With a data rate of $100\,Hz$ at least 2000 data points can be collected, which are stored directly on the SD-card for further data processing. Table I shows the mean values of the relevant axis. The calculated offset and scaling factor of each axis are shown in Table II.

TABLE I
LIS3DH MEASURING DATA AT $\pm 1\,g$

| | x-axis | y-axis | z-axis |
|---|---|---|---|
| $+1\,g$ | 1027.22 | 1026.17 | 1052.20 |
| $-1\,g$ | −1027.96 | −1048.13 | −947.25 |

TABLE II
CORRECTING VALUES OF LIS3DH

| | x-axis | y-axis | z-axis |
|---|---|---|---|
| Offset | $0\,LSB$ | $-11\,LSB$ | $52\,LSB$ |
| Scaling Factor | 0.9965 | 0.9873 | 1.0243 |

### B. Calibration of the gyroscopic sensor

To calibrate the angular rate sensor the IMU platform is placed on a rotating table. The table is driven by a step motor which allows nearly every rotation rate and angular acceleration. For calibration the measuring range is set to $\pm 500\,\frac{^\circ}{s}$ and the data rate to $100\,Hz$.

Similar to the calibration of the acceleration sensor six measuring values are necessary to calibrate the angular rate sensor. Each sensitive axis of the sensor is exposed to a positive and negative rotation. An angular acceleration of $52{,}38\,\frac{°}{s^2}$ was used, so that the rotation rate reaches $500{,}39\,\frac{°}{s}$ after $9{,}55\,s$. This rotation rate is kept for at least $20\,s$. Thereafter, the same procedure is started in the opposite direction. The measured results of the calibration are shown in Table III. The calculated offset and scaling factor of each axis are shown in Table IV.

TABLE III
L3G4200D MEASURING DATA AT $\pm 500.39\,\frac{°}{s}$

| | roll | pitch | yaw |
|---|---|---|---|
| $+500.39\,\frac{°}{s}$ | $29458\,digits$ | $28449\,digits$ | $28533\,digits$ |
| $-500.39\,\frac{°}{s}$ | $-29319\,digits$ | $-28545\,digits$ | $-28391\,digits$ |

TABLE IV
CORRECTING VALUES OF L3G4200D

| | roll | pitch | yaw |
|---|---|---|---|
| Offset | $70\,LSB$ | $-48\,LSB$ | $71\,LSB$ |
| Scaling Factor | 0.9730 | 1.0034 | 1.0046 |

## V. STEP DETECTION RESULTS

For a step detection the acceleration sensor is operated with active high pass filter, that filters out the acceleration of gravity of the measuring data. The angular rate sensor runs without activated high pass filter. The data rate of the two sensors is set to the same value of $100\,Hz$ as used in calibration mode.

Fig. 2 shows the acceleration data of a right-foot mounted IMU on a straight-line path. At around $17.25\,s$ the person wearing the IMU starts to walk. Compared to the peaks at $18.50\,s$ and $19.70\,s$ the first peaks are relatively small. The reason for this fact is that the two feet stand side by side at the beginning. In the following steps the foot with the IMU rests behind the body center and covers a greater distance until the next landing. While starting and landing of the foot the abrupt accelerations are very good recognizable as peaks in the diagram. While the foot is in the air there are only peaks and while it is on the ground there are nearly no recognizable accelerations.

Because a foot mounted system is not practical and not desired for the future application a hip-mounted step-detection should be derived from it. Ideally, the step-detection should work independently from the orientation of the IMU. It is fixed to the belt at the level of the right hip via a belt clip without respect to the same orientation every time. Fig. 3 shows the recorded data set of a straight-line path for the hip-mounted IMU.

When comparing Fig. 2 with Fig. 3 it gets obvious that the accelerations at the foot are more pronounced than at the hip and the clearly resting phase is completely missing. The little peaks at $32.50\,s$, $33.75\,s$ and $35\,s$ are caused by movements of the left leg respectively the left foot. Therefore, the hip-mounted system recognizes twice the number of events.

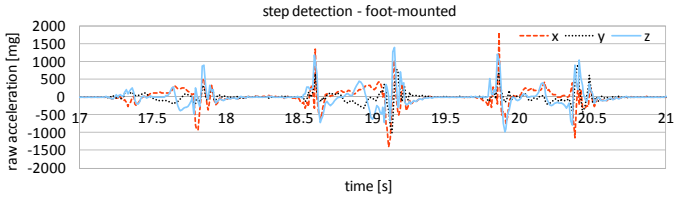


Fig. 2. Step detection for foot-mounted IMU (three axis data of the acceleration sensor).

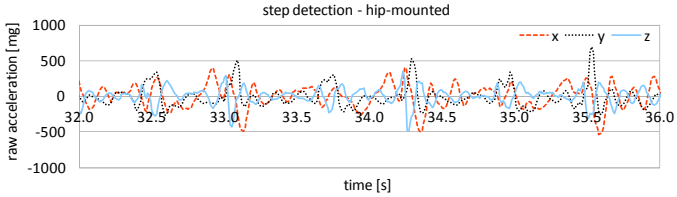


Fig. 3. Step detection for hip-mounted IMU (three axis data of the acceleration sensor).

The fast gradients while the acceleration falls from a local maximum to a local minimum or the other way around are clearly visible. A closer view shows that the gradient has a duration of about seven samples ($70\,ms$). The next step is to find an algorithm that extracts these steps out of the raw data. The first step is to calculate an overall acceleration using (7).

$$a_{mag} = \sqrt{a_x^2 + a_y^2 + a_z^2} \tag{7}$$

Its advantage is that any orientation of the IMU leads to comparable results. Afterwards, (8) is applied to calculate the sum of eight successive overall accelerations.

$$a_{sum} = \sum_{k=1}^{8} a_{mag,k} \tag{8}$$

The idea is to get a local extremum that can be uniquely identified. The above-mentioned steps are applied to the raw data in Fig. 3. The results after the first two steps of the algorithm are shown in Fig. 4. In the next step the algorithm searches over a time period of $480\,ms$ for the minimal and maximal sum value and calculates the mean of them with (9) to generate a dynamic threshold.

$$thres_{dyn} = \frac{a_{sum\_max} + a_{sum\_min}}{2} \tag{9}$$

A step is considered to be detected if the sum of the accelerations is smaller than the previous one and the dynamic threshold. To avoid a multiple step detection, a blocking time

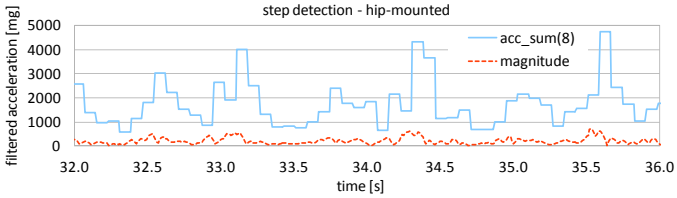


Fig. 4. Step detection for hip-mounted IMU (accumulated sum).

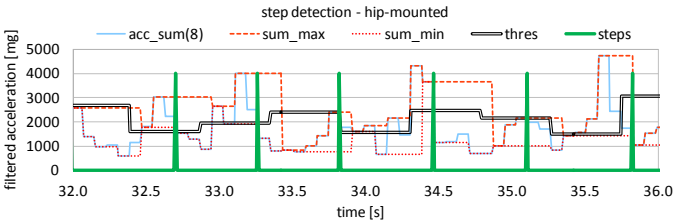


Fig. 5. Step detection for hip-mounted IMU (detected steps).

of $480\,ms$ was applied. During this time no step will be counted even if it meets the requirements. A blocking time of $480\,ms$ has proven to be an acceptable value. Another problem occurs if the IMU is exposed to light vibrations that are triggered by walking on one point. To avoid this problem a step detection is started only if $a_{sum\_min} > 500\,mg$. Fig. 5 shows the data processing of the algorithm. A detected step is visualized through a value of $4000$ in order to uniquely identify the peaks in the figure.

Fig. 6 shows the floor plan of the institute building and the track which was paced out every time. The track is divided into seven sections and a short break was inserted between the sections to uniquely detect these points in the later analysis. Some sections contain stairs while other sections

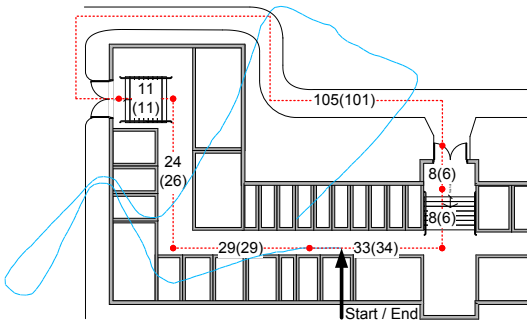


Fig. 6. Floor plan of the test bed, pace out track (red dashed line) and estimated path (solid blue line).

are flat regions inside and outside of the institute building. The numbers represent the steps that are counted from the IMU for the individual segments. The numbers in brackets represent the real steps. There is only a little difference between the two numbers, that shows that the steps are counted relatively reliable. Table V shows an overview over the real steps and the counted steps of the test runs.

TABLE V
COMPARISON BETWEEN REAL AND COUNTED STEPS

| | Counted Steps | (Real Steps) |
|---|---|---|
| Minimum | 212 | (214) |
| Maximum | 215 | (217) |

The direction recognition that only depends on the L3G4200D angular rate sensor is the most challenging issue. Even with a starting calibration an offset error occurs that accumulates to an error of about $30 - 70°$ after completing one round in approximately $210\,s$.

Fig. 6 shows in light blue the real track and in red a combined navigation of the step counter and the rotation rate information. Due to the occurrence of the offset error the real track is very different from that one calculated with the combined navigation. The form can still be guessed but the position is far away from the real value.

## VI. Conclusion and Future Work

The algorithm described in this paper in combination with MEMS-based sensors lead to a reliable step detection. In comparison with a foot-mounted IMU, the hip-mounted IMU is able to detect movements of both legs and not only of one. Within a complete double step this system counts two events. In the experimental setup, 213 out of 216 steps were detected by the step detection framework. The covered distance is calculated using a defined and fixed step length. Thus, in occurrence of stairs, the resulting distance is greater than the real distance.

Further system developments concentrate on improvements of the step detection algorithm containing the detection of a variation of step speeds with an adaption of the step length on the fly. The direction detection based on the angular rate sensor should also be improved. A magnetic field sensor can be used for a sensor fusion with the angular rates to reach a good long-term stability.

At the end an integration of the prototyping platform into an existing RF-based positioning system is desired so that a data fusion can be accomplished.

## References

[1] R. Mautz and S. Tilch, "Survey of optical indoor positioning systems," in *Indoor Positioning and Indoor Navigation (IPIN), 2011 International Conference on*, sept. 2011, pp. 1 –7.

[2] J. Hightower and G. Boriello, "*A survey and taxonomy of location systems for ubiquitous computing*," University of Washington, Department of Computer Science and Engineering, Tech. Rep., 2001.

[3] R. Libby, "A simple method for reliable footstep detection in embedded sensor platforms," Tech. Rep., 2008.

[4] A. Jiménez, F. Seco, C. Prieto, and J. Guevara, "A comparison of pedestrian dead-reckoning algorithms using a low-cost MEMS IMU," in *6th IEEE International Symposium on Intelligent Signal Processing*, 2009, pp. 37–42.

[5] N. Zhao, "Full-featured pedometer design realized with 3-axis digital accelerometer," Analog Devices, Tech. Rep., 2010.

[6] R. Dorobantu and B. Zebhauser, "Field evaluation of a low-cost strapdown imu by means gps," *Ortung und Navigation*, vol. 1, pp. 51– 65, 01 1999.

[7] L. Klingbeil, M. Romanovas, P. Schneider, M. Traechtler, and Y. Manoli, "A modular and mobile system for indoor localization," in *Indoor Positioning and Indoor Navigation (IPIN), 2010 International Conference on*, sept. 2010, pp. 1 –10.

[8] M. De Agostino, A. M. Manzino, and M. Piras, "Performances comparison of different MEMS-based IMUs," in *Position Location and Navigation Symposium (PLANS), 2010 IEEE/ION*, may 2010, pp. 187 –201.

[9] *L3G4200D MEMS motion sensor: ultra-stable three-axis digital output gyroscope, Revision 3*, STMicroelectronics, 2010, l3G4200D.

[10] *LIS3DH MEMS digital output motion sensor ultra low-power high performance 3 -axes, Revision 1*, STMicroelectronics, 2011.

[11] A. Fink and H. Beikirch, "Combining of redundant signal strength readings for an improved RF localization in multipath indoor environments," in *15th International Conference on Information Fusion*, 2012, pp. 1–7.

[12] *AVR122: Calibration of the AVR's internal temperature reference*, Rev. 8108a-avr-02/08 ed., Atmel Corporation, 2008.